Chen *et al. Clinical Proteomics* (2026) 23:30
https://doi.org/10.1186/s12014-026-09606-3

Clinical Proteomics

RESEARCH Open Access

Plasma proteomics of extracellular vesicles identifies key proteins correlating to postoperative atrial fibrillation after coronary artery bypass surgery

Huan-Xin Chen[1,2], Qin Yang[1,2] and Guo-Wei He[1,2,3*]

Abstract

Background New-onset postoperative atrial fibrillation (POAF) after coronary artery bypass grafting (CABG) is a major complication and the precise mechanism remains unclear. EVs have become a special intercellular information transmission system secreted from different cells. The present study aimed to identify differentially expressed proteins (DEPs) of the plasma exosomes (Extracellular Vesicles, EVs) from patients with POAF after CABG and explored the pathogenesis of POAF.

Methods Label-free quantitative LC–MS/MS proteomics analyses were performed to find changes in protein levels proteomic alterations in plasma EVs of patients with POAF ($n=6$) after CABG and sinus rhythm (SR, $n=6$). The DEPs screened by bioinformatics analysis were validated by parallel reaction monitoring (PRM) quantitative analysis from a new set of plasma samples (POAF $n=9$; SR $n=9$).

Results Exosomal proteomics identified 51 significant DEPs including 29 up-regulated and 22 down-regulated proteins in POAF group compared to the SR control. Bioinformatics analysis showed that the DEPs were significantly enriched in cysteine and methionine metabolism, Toll-like receptor signaling pathway, AGE-RAGE signaling pathway in diabetic complications and Diabetic cardiomyopathy. The PRM reconfirmed that serum amyloid P-component and Collagen alpha-2(I) chain were significantly down-regulated in POAF group.

Conclusions This study provides a new insight into the exploration of the pathogenesis of POAF. Abnormally expressed SAP and Collagen alpha-2(I) chain correlate to POAF and might be further explored for their role in the occurrence of POAF. These two proteins in the plasma EVs may be developed as biomarkers for future diagnosis and treatment of POAF in the clinical setting.

Keywords Postoperative atrial fibrillation, Coronary artery bypass grafting, Proteomics, Extracellular Vesicles, Serum amyloid P-component, Collagen alpha-2(I) chain

*Correspondence:
Guo-Wei He
gwhezj@163.com; gwhe@tju.edu.cn
[1]Department of Cardiovascular Surgery & The Institute of Cardiovascular Diseases, TEDA International Cardiovascular Hospital, Tianjin University & Chinese Academy of Medical Science, Tianjin 300457, China
[2]Tianjin Key Laboratory of Molecular Regulation of Cardiovascular Diseases and Translational Medicine, 300457 Tianjin, China
[3]Division of Cardiothoracic Surgery, Department of Surgery, Oregon Health & Science University, Portland, OR 97239-3098, USA

Background

Coronary heart disease is the single most common cause of death throughout the world for both men and women [1]. Coronary artery bypass grafting (CABG) is the best method and the primary surgical treatment for multivessel coronary heart disease [2]. New-onset postoperative atrial fibrillation (POAF) after CABG is one of the major complications, with an incidence of about 20% to 50% [3]. The risk factors for POAF after CABG include age, sex, body mass index, chronic obstructive pulmonary disease, cardiopulmonary bypass surgery, heart valve disease, epicardial adipose tissue, and obstructive sleep apnea [4, 5]. The precise mechanism of POAF after CABG remains unclear.

Extracellular Vesicles (EVs) are membrane vesicles secreted from different cells, typically 40–160 nm in diameter (average 100 nm) [6, 7]. EVs are widely present in various body fluids including blood, ascites, cerebrospinal fluid and urine, and carry proteins, lipids, nucleic acids (DNA, mRNA, lncRNA, miRNA, and circRNA) and other biological macromolecules [8].

Recent studies have shown that EVs have become a special intercellular information transmission system, which not only affects the physiological state of cells, but also is closely related to the occurrence and development of many diseases, including coronary heart disease in particular [9–12]. It has been demonstrated that EVs, circulating or released from heart tissue, are actively involved in cardiac remodeling in response to stress factors [13]. EVs released from progenitor/stem cells have protective effects in heart diseases and have shown potential for regeneration in the heart [13]. In addition, EVs from adipose-derived stem cells play an increasingly important role in cardiovascular diseases in terms of the impact of macrophage polarization and the endothelial, antiapoptosis, and angiogenesis effects [14]. As mediators of intercellular communication, platelet EVs play a key role in atherosclerotic thrombosis in regulating coagulation, inflammation, angiogenesis and mediating endothelial cell dysfunction and apoptosis [15, 16]. Exosomal miRNAs delivery has been implicated in cardiac regeneration and protection and EVs containing miRNAs can be clinically useful in cell-free therapeutic approaches and can serve as prognostic and diagnostic biomarkers for AF [17]. Exosomal miR-320d has been associated with cardiomyocyte apoptosis and cell viability in AF, and the effect of miR-320d on cardiomyocytes relies on STAT3 [18].

Proteins from plasma EVs may act as biomarkers to reflect the physiological status and pathological conditions induced by AF. The aim of the present study was to identify differentially expressed proteins (DEPs) of plasma EVs in patients with POAF or sinus rhythm (SR) after CABG, using label-free quantitative LC–MS/MS proteomics analyses. Such DEPs may become potential biomarkers for predicting POAF and facilitate the therapeutic targets and for a better understanding of the molecular mechanisms of POAF after CABG.

Materials and methods

Patients

In this study, a total of 30 patients with POAF (n = 15) and SR (n = 15) after CABG were recruited. Twelve patients (6 vs. 6) were allocated to the discovery set and 18 (9 vs. 9) to the validation set (Fig. 1A). POAF was defined as multiple AF lasting > 30 s, recorded by electrocardiogram monitor or continuous wireless rhythmic monitoring, began immediately after surgery or later before discharge, requiring anti-AF treatment (usually at least one intravenous injection of intravenous amiodarone) [5, 19].

All participants had sinus rhythm before surgery, underwent CABG for the first time and were matched by ethnicity, gender, age and clinical characteristics, including body mass index, smoking, hypertension, myocardial infarction, left ventricular ejection fraction and cardiopulmonary bypass. An informed consent form was obtained from the patient. The study protocol conforms to the ethical guidelines of the 1975 Declaration of Helsinki and has been approved by the Ethics Committee (Internal Review Board) of TEDA-international Cardiovascular Hospital, Tianjin, China ([2022]-0429-5).

EVs isolation

Blood samples were harvested by venipuncture from all patients in the fasting state before the day of surgery. The plasma was separated by centrifugation at 1,500×g for 10 min and stored at -80˚C for EVs isolation.

EVs from plasma samples were collected using exosome extraction and purification kit (Umibio, UR52136, China) according to the manufacturer's instructions. Briefly, plasma samples were thawed and centrifuged at 3,000×g for 10 min to remove cellular debris, then centrifuged at 10,000×g for 20 min to remove impurities. The supernatant was collected and diluted with precooled 1×PBS, followed by Blood PureExo Solution, vortexed 1 min and incubated for up to 120 min. Subsequently, the mixtures were centrifuged at 10,000×g for 60 min to precipitate exosome pellets. Pellets were resuspensed with 1×PBS and purified with Exosome Purification Filter at 3,000×g for 10 min. All above procedures were performed at 4℃. All extracted EVs were stored at -80℃ immediately.

The typical membrane morphology, particle size, and concentration was measured using transmission electron microscopy (TEM, JEOL-1230, Japan) and nanoparticle tracking analysis (NTA, ZetaView PMX-110, Germany) to validate the isolation and purification of EVs.

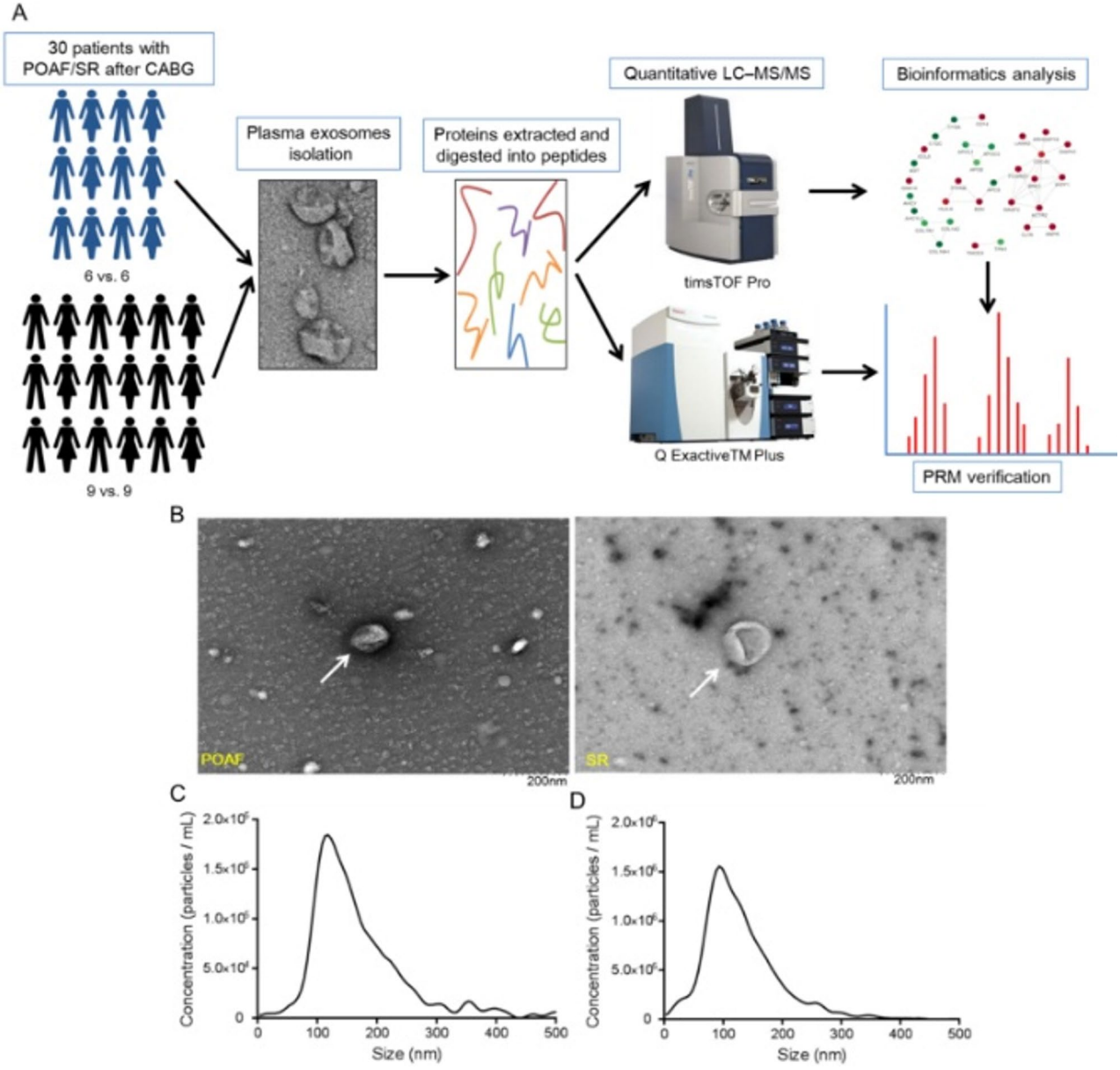

Fig. 1 The main workflow in the present study and the characterization of EVs isolated from plasma of patients with POAF and SR after CABG. (**A**) Schematic of the workflow used for the proteomics analysis of plasma EVs in POAF/SR patients. (**B**) TEM images of membrane vesicles of EVs. The arrow indicates the EVs. Scale Bar: 200 nm. (**C**-**D**) Representative NTA of isolated EVs from POAF (**C**) and SR(D). Most vesicles had a size of 100–200 nm in diameter

Quantitative proteomics analysis of EVs

The exosome samples were mixed with lysate of equal volume and placed on ice for 10 min for cleavage. After centrifugation at 12,000×g for 5 min, the concentration of protein existed in supernatant was determined with BCA kit.

The above protein solution was reduced with 5mM dithiothreitol for 30 min at 56 °C and alkylated with 11 mM iodoacetamide for 15 min at room temperature in darkness. The protein sample was then diluted by adding 100mM TEAB to the urea concentration of less than 2 M. Trypsin was added at a ratio of 1:50 trypsin/protein mass in the first overnight digestion and 1:100 in the second 240 min digestion. The peptides were then desalinated using C18 SPE column. Quantitative analysis of peptides by LC-MS/MS were performed in Jingjie PTM Biolab Co. Ltd (Hangzhou, China). The relative expression ratio of POAF/SR > 1.5 or < 1/1.5 and P value < 0.05 was regarded as DEPs.

Bioinformatics analysis

Subcellular localization of DEPs was predicted using the software wolfpsort, an updated version of PSORT/PSORT II for eukaryotic sequence prediction. Identified

proteins domain functional description were annotated by InterProScan, which analyses the data through both the InterPro domain database (http://www.ebi.ac.uk/interpro/) and the protein sequence alignment.

Gene Ontology (GO) annotation proteome was derived from the UniProt-GOA database (http://www.ebi.ac.uk/GOA/). The proteins were classified by Gene Ontology annotation based on three categories: biological process, cellular component and molecular function. The Kyoto Encyclopedia of Genes and Genomes (KEGG) database (http://www.genome.jp/kegg/) was used to annotate the pathway of protein involved. Firstly, using KEGG online service tools KAAS to annotate protein's KEGG database description. The annotation results were then mapped on the KEGG pathway database by the KEGG mapper. For each class or pathway, a two-tailed Fisher's exact test was used to examine the enrichment of DEPs against all identified proteins. The corrected p value < 0.05 is considered significant. The protein–protein interaction network (PPI) of all DEPs was generated based on the STRING database (http://string-db.org/), with confidence scores greater than 0.7.

Parallel reaction monitoring (PRM) quantitative analysis

PRM is a high throughput method of targeted quantification based on high resolution and high mass accuracy mode on a mass spectrometer [20]. To validate the results of label-free proteomics, the DEPs screened by bioinformatics analysis were further tested by PRM quantitative analysis from a new set of plasma samples (POAF n = 9; SR n = 9). The protocol for EVs isolation and protein digestion was the same as described above. The tryptic peptides were isolated at a constant flow rate of 500 nL/min on the EASYnLC 1000 UPLC system. The peptides were subjected to NSI source followed by tandem mass spectrometry (MS/MS) in Q ExactiveTM Plus coupled online to the UPLC. The applied electrical voltage was 2.1 kV. A full scan with m/z ranging from 425 to 1060 detected intact peptides in Orbitrap at a resolution of 70,000. Peptides were then selected for MS/MS using a normalized collision energy setting of 27, and the fragments were detected in Orbitrap at a resolution of 17,500. A data-independent procedure that alternated between one MS scan followed by 20 MS/MS scans. Automatic gain control was set at 3E6 for full MS and 1E5 for MS/MS. The maximum IT was set to 50 ms for full MS and auto for MS/MS. The isolation window for MS/MS was set to 1.6 m/z.

Receiver operating characteristics (ROC) analysis

The ROC analysis was performed to assess the sensitivity and specificity of DEPs for POAF, using the relative expression of DEPs from label-free and PRM quantitative proteomics assays. The area under the ROC curve (AUC) above 0.70 was known as the acceptable range for evaluating the useful biomarkers.

Statistical analysis

GraphPad Prism (version 6.01) were used for statistical analysis. Data are expressed as mean ± SEM. Intergroup comparisons were performed using two-tailed Fisher's exact test. The p-value less than 0.05 were considered as statistically significant.

Results

Isolation and characterization of the plasma EVs

The plasma EVs derived from the patients with POAF or SR after CABG were analyzed by TEM and NTA. Fig. 1B shows that the size of EVs falls into the typical range, as well as the normal morphology of membrane vesicles with lipid bilayers. The NTA revealed that the diameter size distribution of these EVs varies from 30 nm to 200 nm (Fig. 1C). These results indicated that EVs were successfully isolated from the plasma samples.

Proteome profiling of plasma EVs

The mass spectrometry and database search identified 788,162 total spectrums, 142,907 matched spectrums, 10,915 peptides, 9589 unique peptides, 1470 proteins and quantified 1301 proteins (Fig. 2A). In contrast to the SR group, 51 significantly DEPs including 29 up-regulated proteins and 22 down-regulated proteins in the POAF group were shown in a volcano plot (Table 1; Fig. 2B). The cluster heatmap illustrated the relative expressions and relationships between all significantly DEPs and PRM-validated DEPs (Fig. 2C-D).

Functional classification and PPI network analysis of DEPs

Functional classification analysis on 51 DEPs was performed based on subcellular location and GO. The subcellular localization predication software WoLF PSORT was used and the results suggested that the DEPs were mainly located in cytoplasm (39.22%), extracellular (35.29%) and nucleus (9.8%) (Fig. 3A).

GO classification analysis showed that the DEPs were significantly enriched in cellular process (90%), biological regulation (80%) and response to stimulus (74%) of biological processes (BP); in intracellular (86%), cell (86%) and protein-containing complex (54%) of cellular components (CC); in binding (74%), catalytic activity (30%) and structural molecule activity (18%) of molecular functions (MF) (Fig. 3B).

The PPI network was created using the STRING website and visualized by R package networkD3. Figure 3C displayed the correlation for each of the DEPs in this study.

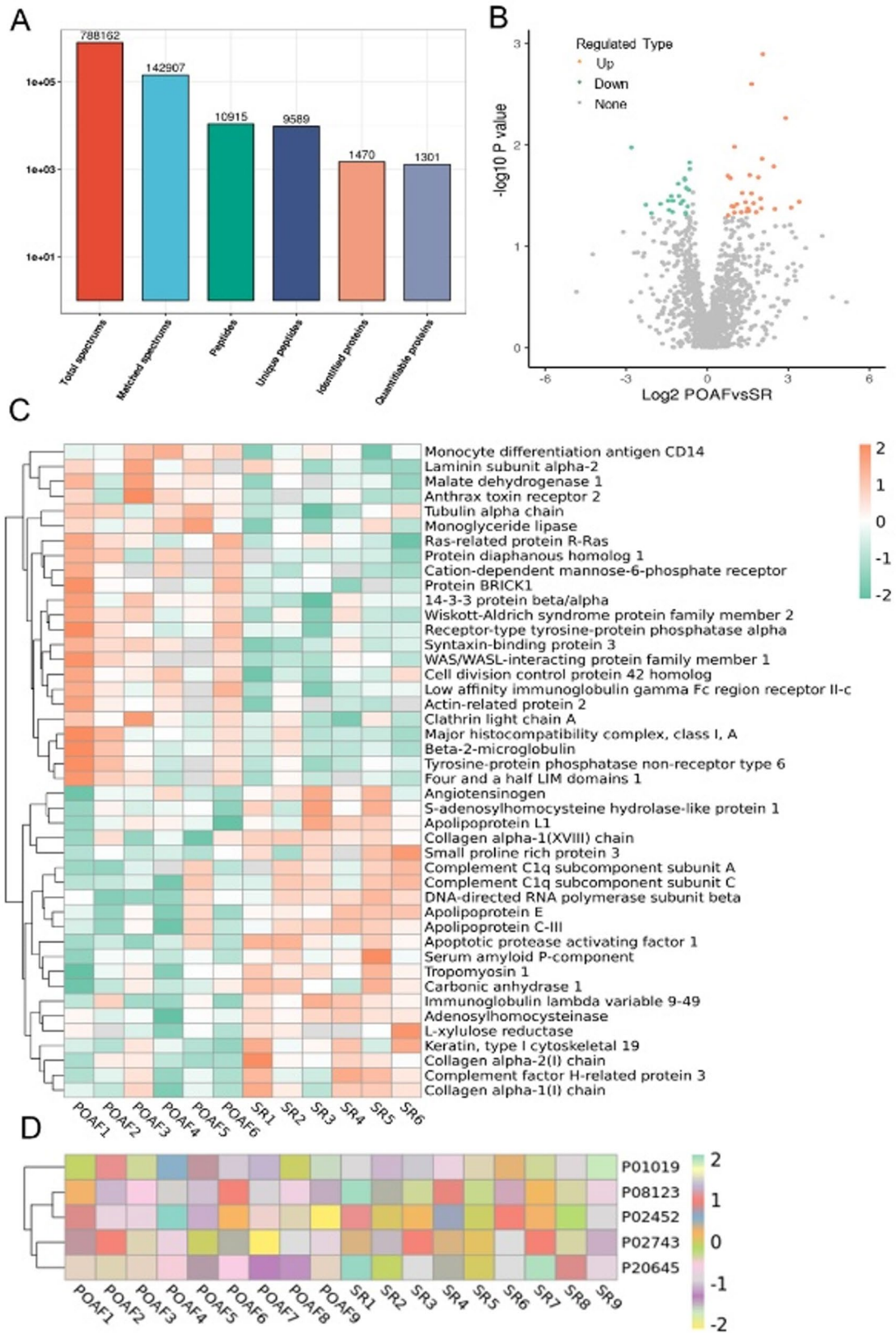

Fig. 2 Protein identification and quantitative evaluation of plasma derived EVs. (**A**) The results distribution diagram of LC-MS/MS. (**B**) The volcano plots showing significantly differential expressed proteins include 29 up-regulated proteins and 21 down-regulated proteins based on fold changes (> 1.5 or < 0.667, $p < 0.05$). (**C**-**D**) The heatmap plots of DEPs

Table 1 All 51 DEPs identified by label-free quantitative proteomics in the present study

Protein accession	Protein name	Gene name	POAF/SR Ratio	POAF/SR *P* value
C9JLV4	Apoptotic protease-activating factor 1	APAF1	0.143	0.011
B1AN48	Small proline-rich protein 3 (Fragment)	SPRR3	0.207	0.039
J3KS22	L-xylulose reductase (Fragment)	DCXR	0.238	0.047
P02743	Serum amyloid P-component	**APCS**	0.301	0.038
X6RLJ0	Complement C1q subcomponent subunit A (Fragment)	C1QA	0.367	0.036
P02747	Complement C1q subcomponent subunit C	C1QC	0.375	0.044
P39060	Collagen alpha-1(XVIII) chain	COL18A1	0.397	0.032
O43865	S-adenosylhomocysteine hydrolase-like protein 1	AHCYL1	0.411	0.046
P28072	Proteasome subunit beta type-6	PSMB6	0.415	0.036
P08727	Keratin, type I cytoskeletal 19	KRT19	0.476	0.024
Q02985	Complement factor H-related protein 3	CFHR3	0.484	0.032
P01019	Angiotensinogen	AGT	0.506	0.038
P23526	Adenosylhomocysteinase	AHCY	0.537	0.036
P02656	Apolipoprotein C-III	APOC3	0.559	0.021
C9J4M6	DNA-directed RNA polymerase subunit beta	POLR2B	0.563	0.022
O14791	Apolipoprotein L1	APOL1	0.575	0.047
P00915	Carbonic anhydrase 1	CA1	0.58	0.049
P08123	Collagen alpha-2(I) chain	**COL1A2**	0.584	0.027
P02452	Collagen alpha-1(I) chain	COL1A1	0.604	0.041
Q6ZN40	Tropomyosin 1 (Alpha), isoform CRA_f	TPM1	0.623	0.028
A0A0B4J1Y8	Immunoglobulin lambda variable 9–49	IGLV9-49	0.635	0.015
P02649	Apolipoprotein E	APOE	0.638	0.017
P31946	14-3-3 protein beta/alpha	YWHAB	1.698	0.020
P10301	Ras-related protein R-Ras	RRAS	1.704	0.050
P60953	Cell division control protein 42 homolog	CDC42	1.815	0.021
P04439	HLA class I histocompatibility antigen, A alpha chain	HLA-A	1.879	0.040
P58335	Anthrax toxin receptor 2	ANTXR2	1.969	0.041
P61769	Beta-2-microglobulin	B2M	2.004	0.046
H0YGT0	Low affinity immunoglobulin gamma Fc region receptor II-c	FCGR2C	2.011	0.010
P12236	ADP/ATP translocase 3	SLC25A6	2.144	0.038
O95837	Guanine nucleotide-binding protein subunit alpha-14	GNA14	2.394	0.046
B8ZZ51	Malate dehydrogenase, cytoplasmic	MDH1	2.448	0.030
P29350	Tyrosine-protein phosphatase non-receptor type 6	PTPN6	2.665	0.037
Q9NYL9	Tropomodulin-3	TMOD3	2.771	0.046
P24043	Laminin subunit alpha-2	LAMA2	2.826	0.042
P08571	Monocyte differentiation antigen CD14	CD14	2.919	0.045
Q9Y6W5	Wiskott-Aldrich syndrome protein family member 2	WASF2	2.972	0.020
Q99685	Monoglyceride lipase	MGLL	3.104	0.030
P20645	Cation-dependent mannose-6-phosphate receptor	M6PR	3.124	0.003
P18433	Receptor-type tyrosine-protein phosphatase alpha	PTPRA	3.279	0.038
P09496	Clathrin light chain A	CLTA	3.511	0.046
C9J2C0	Tubulin alpha chain (Fragment)	TUBA8	3.709	0.021
O95865	N(G), N(G)-dimethylarginine dimethylaminohydrolase 2	DDAH2	3.922	0.034
Q8WUW1	Protein BRICK1	BRK1	4.01	0.042
H9KV28	Protein diaphanous homolog 1	DIAPH1	4.078	0.014
O00186	Syntaxin-binding protein 3	STXBP3	4.158	0.001
P61160	Actin-related protein 2	ACTR2	5.505	0.016
P13501	C-C motif chemokine 5	CCL5	5.663	0.043
O43516	WAS/WASL-interacting protein family member 1	WIPF1	7.473	0.005
Q5JXI8	Four and a half LIM domains protein 1 (Fragment)	FHL1	8.614	0.042
Q8N392	Rho GTPase-activating protein 18	ARHGAP18	10.559	0.036

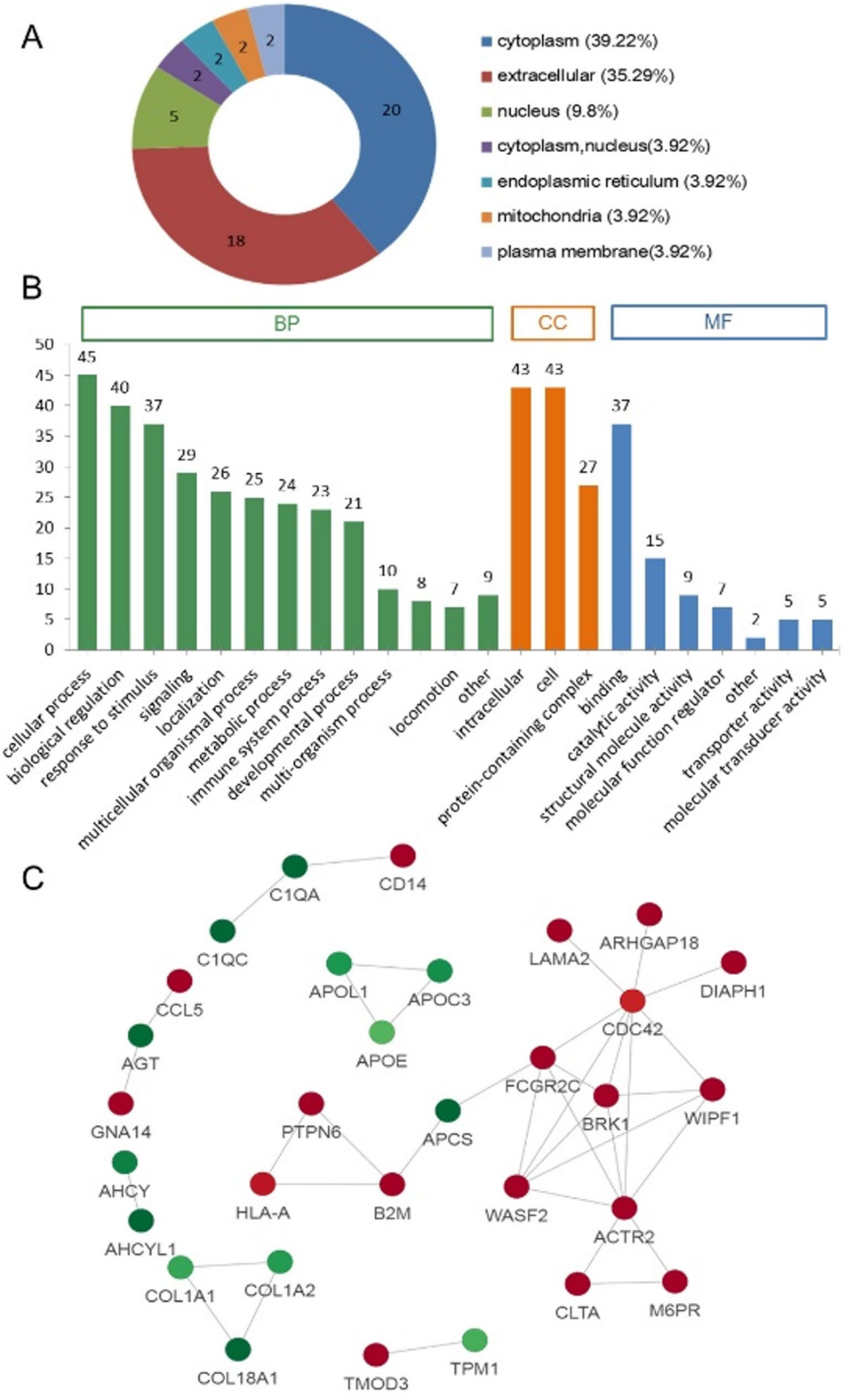

Fig. 3 Functional classification and protein-protein interaction analysis of DEPs. (**A**) Subcellular distribution of DEPs. (**B**) GO classification analysis of DEPs based on three categories: biological process (BP), cellular component (CC) and molecular function (MF). (**C**) PPI analysis of DEPs. Green circles represent down-regulated proteins and red circles represent up-regulated proteins. The darker the color, the larger the difference of DEPs between POAF and SR group

Functional enrichment analysis of DEPs by KEGG and GO

KEGG analysis revealed that 51 DEPs were involved in multiple signal pathways, mainly including cysteine and methionine metabolism (hsa00270), Toll-like receptor signaling pathway (hsa04620), AGE-RAGE signaling pathway in diabetic complications (hsa04933), and Diabetic cardiomyopathy (hsa05415) (Fig. 4A).

The significant GO terms enrichment were analyzed in DEPs. Among BP, DEGs were distributed to striated muscle cell development/differentiation, muscle cell development, cardiovascular system development, and intracellular signal transduction. In CC, DEGs belonged to striated muscle thin filament, myofilament, and banded collagen fibril. In MF, DEGs were responsible for profilin binding, protein tyrosine phosphatase activity and protein phosphorylated amino acid binding (Fig. 4B-D).

The significant difference of serum amyloid P-component (SAP) and collagen alpha-2(I) chain confirmed by PRM quantitative and ROC analysis

The other 18 plasma samples (POAF $n=9$; SR $n=9$) of a new cohort were collected to verify the change of DEGs by PRM. A total of 51 DEPs were initially identified. Twenty of them were chosen for further validation by using PRIM based on the potential correlation to AF. Finally, 6 of which were successfully validated. Among those, the changes of two proteins - SAP (gene name: APCS) and Collagen alpha-2(I) chain (gene name: COL1A2) in AF were consistent with the results of label-free quantification. Figure 4E shows the relative abundance of SAP and Collagen alpha-2(I) chain in label-free and PRM quantitative proteomics (p value < 0.05).

The ROC analysis shows the correlation of SAP (AUC: 0.75; 95% CI: 0.57–0.94; P: 0.03) and Collagen alpha-2(I) chain (AUC: 0.75; 95% CI: 0.56–0.94; P value: 0.03) to POAF, suggesting that the two DEPs are potential diagnostic biomarkers (Fig. 4F).

Discussion

The present study for the first time in a plasma exosomal proteomics analysis in the CABG patients with either POAF or SR found that (1) 51 significantly DEPs were identified in plasma EVs of POAF patients; (2) the significant down-regulation of SAP and Collagen alpha-2(I) chain was confirmed by PRM quantitative analysis in the new cohort; (3) the abnormal expression of SAP and Collagen alpha-2(I) chain affects the interaction with type IV collagen, producing structural defects in collagen. This is associated with the pathogenesis of POAF. Further, the down-regulation of SAP and Collagen alpha-2(I) chain may be developed as potential biomarkers for POAF.

The DEPs verified by both label-free and PRM quantitative proteomics were SAP and Collagen alpha-2(I) chain. Both AUC above 0.7 indicate that the specificity and sensitivity of these two proteins in the plasma EVs satisfy the requirement as biomarkers for POAF.

SAP is a member of the pentaxin family of proteins involved in the resolution of infectious diseases, autoimmunity, and amyloidosis [21]. The amino acid sequence and protein structure of SAP are similar to C-reactive protein [22]. Iodine-123 labelled SAP is used as a diagnostic marker for the diagnosis of systemic amyloidosis [23]. In the cardiovascular system, SAP has been defined as the culprit in amyloidosis in the heart [24]. Atrial arrhythmias and conduction abnormalities are frequently observed in patients with cardiac amyloidosis [25]. SAP can bind to extracellular matrix components such as type IV collagen, proteoglycans, and fibronectin, protect them from digestion by extracellular matrix proteases and by altering the turnover rate and the structure of the basement membrane, playing an important role in determining the structure of those basement membranes [26, 27]. In fact, one of our previously studies indicated that up-regulation of type IV collagen may also be a characteristic feature of AF in rheumatic mitral valve disease [28].

Collagen alpha-2(I) chain (Collagen Type I Alpha 2 Chain) is one of the key subunits of collagen Type I, which is a major cardiac extracellular matrix protein and the defining component of fibrotic depositions [29]. Low expression of Collagen alpha-2(I) chain or COL1A2 with mutations may result in a reduced amount of normal type I collagen and produce structural defects in the collagen molecule [30]. Abnormal deposition of myocardial collagen type-I is associated with higher AF prevalence, incidence, and recurrence after ablation [31].

The most important features of AF are electrical, contractile, and structural remodeling of the atria [32]. Our previous studies have suggested that derangements in the regulation of energy metabolites caused by abnormal proteins expression in the PPAR pathway are closely related to the occurrence of AF [33, 34]. In the present study, we identified significantly decreased SAP and Collagen alpha-2(I) chain from the plasma EVs of POAF patients. We illustrated a schema to explain the pathlogical roles of thes two proteins (Fig. 5). Low expression of SAP causes cardiac amyloidosis, which is complicated with atrial arrhythmias and conduction abnormalities, and interacted with type IV collagen, resulting in abnormal basement membranes [22–29]. In addition, low expression of Collagen alpha-2(I) chain produces structural defect of collagen, which is associated with higher AF prevalence [32].

The sample size of this study is limited due to the expensive and complex omics studies that usually involve limited samples, particularly in exosomal proteomics. The results from this exosomal proteomics study have

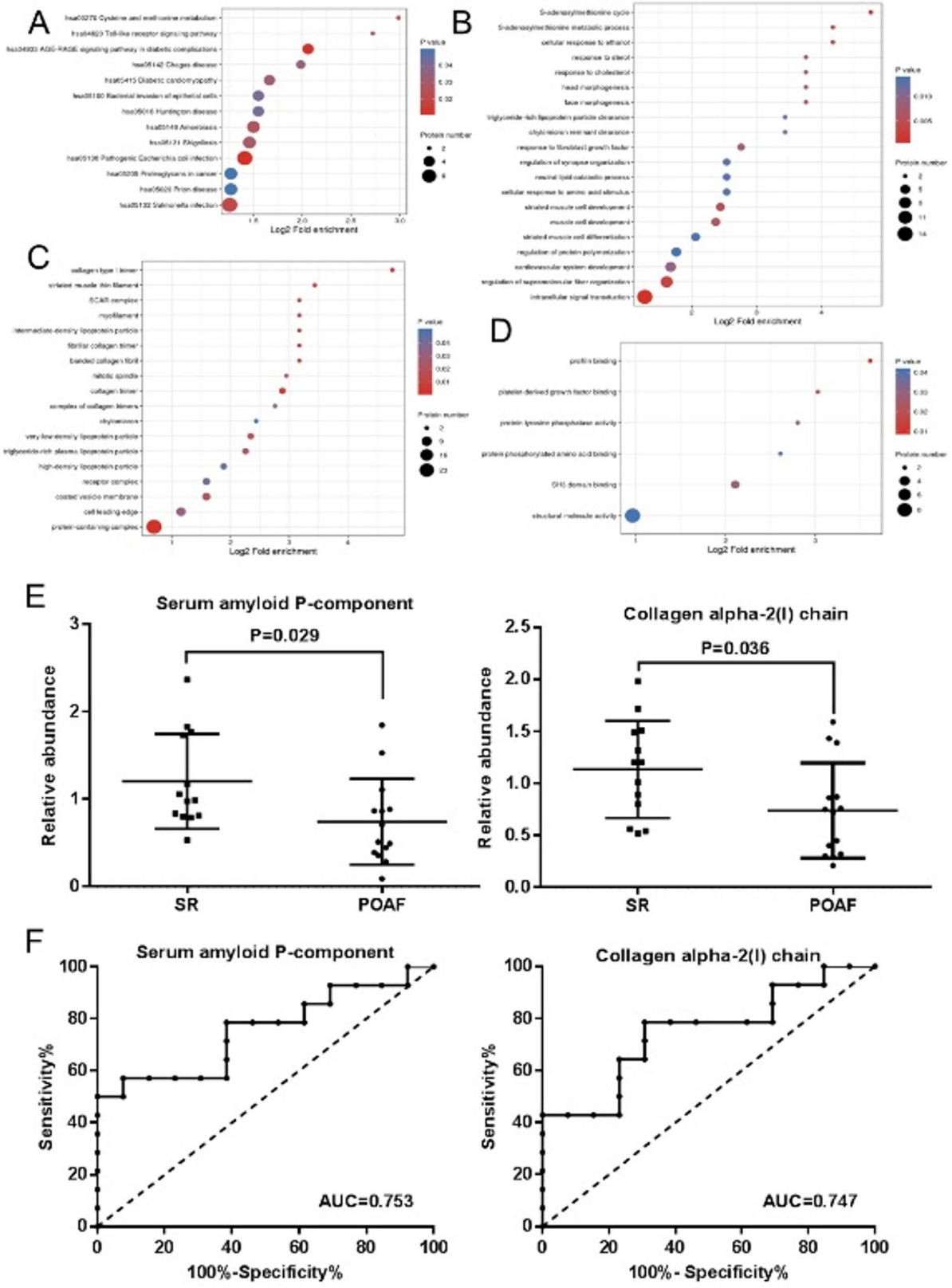

Fig. 4 Functional enrichment analysis, PRM verification and ROC analysis of DEPs. (**A**) KEGG pathway analysis. (**B**) Functional enrichment analysis of BP. (**C**) Functional enrichment analysis of CC. (**D**) Functional enrichment analysis of MF. (**E**) Relative abundance of Serum amyloid P-component and Collagen alpha-2(I) chain in label-free and PRM quantitative proteomics. (**F**) The ROC curves of the potential diagnostic biomarkers (Serum amyloid P-component and Collagen alpha-2(I) chain) for POAF compared with SR based on the results of label-free and PRM quantitative proteomics

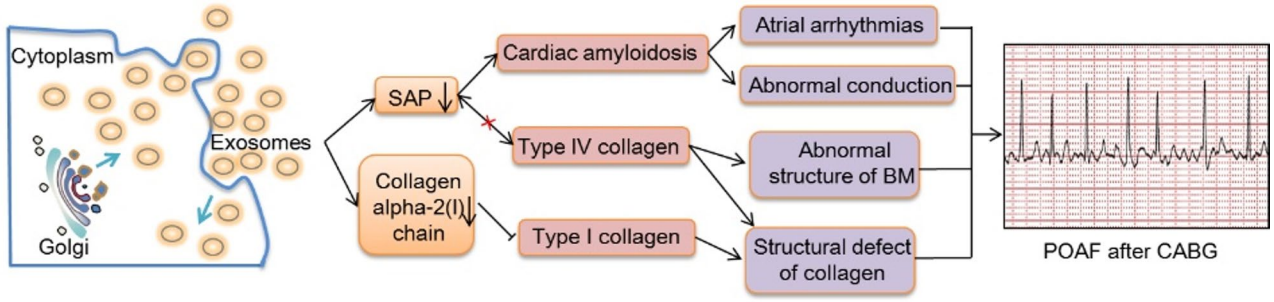

Fig. 5 The schema describing the involvement of the exosomal proteins SAP and Collagen alpha-2(I) chain in the pathogenesis of POAF after CABG

given useful information for the exosomal biomarkers for POAF.

Conclusion

In conclusions, this study provides a new insight into the exploration of the pathogenesis of POAF. Abnormally expressed SAP and Collagen alpha-2(I) chain correlate to POAF and might be further explored for their role in the occurrence of POAF. These two proteins in the plasma EVs may be developed as biomarkers for future diagnosis and treatment of POAF in the clinical setting.

Abbreviations

CABG	Coronary artery bypass grafting
POAF	Postoperative atrial fibrillation
EVs	Extracellular Vesicles
SR	Sinus rhythm
DEPs	Differentially expressed proteins
TEM	Transmission electron microscopy
NTA	Nanoparticle tracking analysis
GO	Gene Ontology
KEGG	Kyoto Encyclopedia of Genes and Genomes
PPI	Protein–protein interaction network
PRM	Parallel reaction monitoring
ROC	Receiver operating characteristics
AUC	Area under the ROC curve
BP	Biological processes
CC	Cellular components
MF	Molecular functions
SAP	Serum amyloid P-component

Acknowledgements

Not applicable.

Author contributions

HXC: data curation, formal analysis, investigation, validation, and writing-original draft; QY: data curation and formal analysis; GWH: conceptualization, data curation, formal analysis, funding acquisition, methodology, project administration, supervision, visualization, writing-review and editing; all authors read and approved the final manuscript.

Funding

This work was supported by the National Natural Science Foundation of China [82370350 & 82170353]; Tianjin Municipal Heath Commission [TJWJ2025MS062]; Tianjin Key Medical Discipline Construction Project [TJYXZDXK-3–036 C] and Special Fund for High Quality Development Project.

Data availability

The mass spectrometry proteomics data have been deposited to the ProteomeXchange Consortium (https://proteomecentral.proteomexchange.org) via the iProX partner repository with the dataset identifier PXD071850.

Declarations

Ethics approval and consent to participate

The informed consent form was obtained from the patients with POAF after CABG and sinus rhythm. The plasma samples of all participants were processed following the protocol and approved by the Ethics Committee of TEDA-international Cardiovascular Hospital, Tianjin, China ([2022]-0429-5).

Consent for publication

Not applicable.

Competing interests

The authors declare no competing interests.

Received: 11 February 2025 / Accepted: 7 April 2026
Published online: 24 April 2026

References

1. Gaziano TA, Bitton A, Anand S, Abrahams-Gessel S, Murphy A. Growing epidemic of coronary heart disease in low- and middle-income countries. Curr Prob Cardiol. 2010;35(2):72–115.
2. Mahmoud S, Shahin M, Yousif N, Denegri A, Abo DL, Luscher TF. Cardiovascular risk profile, presentation and management outcomes of patients with acute coronary syndromes after coronary artery bypass grafting. Curr Prob Cardiol. 2022;47(11):101078.
3. Gorenek B, Pelliccia A, Benjamin EJ, Boriani G, Crijns HJ, Fogel RI, et al. European Heart Rhythm Association (EHRA)/European Association of Cardiovascular Prevention and Rehabilitation (EACPR) position paper on how to prevent atrial fibrillation endorsed by the Heart Rhythm Society (HRS) and Asia Pacific Heart Rhythm Society (APHRS). Eur J Prev Cardiol. 2017;24(1):4–40.
4. Thoren E, Wernroth ML, Christersson C, Grinnemo KH, Jideus L, Stahle E. Compared with matched controls, patients with postoperative atrial fibrillation (POAF) have increased long-term AF after CABG, and POAF is further associated with increased ischemic stroke, heart failure and mortality even after adjustment for AF. Clin Res Cardiol. 2020;109(10):1232–42.
5. Li XY, Hou HT, Chen HX, et al. Preoperative plasma biomarkers associated with atrial fibrillation after coronary artery bypass surgery. J Thorac Cardiov Sur. 2021;162(3):851–63.
6. Hassanzadeh A, Rahman HS, Markov A, Endjun JJ, Zekiy AO, Chartrand MS, et al. Mesenchymal stem/stromal cell-derived exosomes in regenerative medicine and cancer; overview of development, challenges, and opportunities. Stem Cell Res Ther. 2021;12(1):297.
7. Kalluri R, LeBleu VS. The biology, function, and biomedical applications of exosomes. Science. 2020; 367(6478):eaau6977.
8. Thakur A, Parra DC, Motallebnejad P, Brocchi M, Chen HJ, Exosomes. Small vesicles with big roles in cancer, vaccine development, and therapeutics. Bioact Mater. 2022;10:281–94.
9. Emanueli C, Shearn AI, Angelini GD, Sahoo S. Exosomes and exosomal miRNAs in cardiovascular protection and repair. Vasc Pharmacol. 2015;71:24–30.
10. Hulsmans M, Holvoet P. MicroRNA-containing microvesicles regulating inflammation in association with atherosclerotic disease. Cardiovasc Res. 2013;100(1):7–18.

11. Melo SA, Sugimoto H, O'Connell JT, Kato N, Villanueva A, Vidal A, et al. Cancer exosomes perform cell-independent microRNA biogenesis and promote tumorigenesis. Cancer Cell. 2014;26(5):707–21.
12. He C, Zheng S, Luo Y, Wang B. Exosome Theranostics: Biology and Translational Medicine. Theranostics. 2018;8(1):237–55.
13. Patil M, Henderson J, Luong H, Annamalai D, Sreejit G, Krishnamurthy P. The art of intercellular wireless communications: exosomes in heart disease and therapy. Front Cell Dev Biol. 2019;7:315.
14. Zhou F, Li K, Yang K. Adipose-derived stem cell exosomes and related microRNAs in Atherosclerotic cardiovascular disease. J Cardiovasc Transl. 2023;16(2):453-462.
15. Li J, Tan M, Xiang Q, Zhou Z, Yan H. Thrombin-activated platelet-derived EVs regulate endothelial cell expression of ICAM-1 via microRNA-223 during the thrombosis-inflammation response. Thromb Res. 2017;154:96–105.
16. Huber HJ, Holvoet P. Exosomes: emerging roles in communication between blood cells and vascular tissues during atherosclerosis. Curr Opin Lipidol. 2015;26(5):412–9.
17. Hao H, Dai C, Han X, Li Y. A novel therapeutic strategy for alleviating atrial remodeling by targeting exosomal miRNAs in atrial fibrillation. Bba-Mol Cell Res. 2022;1869(12):119365.
18. Liu L, Zhang H, Mao H, Li X, Hu Y. Exosomal miR-320d derived from adipose tissue-derived MSCs inhibits apoptosis in cardiomyocytes with atrial fibrillation (AF). Artif Cells Nanomed Biotechnol. 2019;47(1):3976–84.
19. Montaigne D, Marechal X, Lefebvre P, Modine T, Fayad G, Dehondt H, et al. Mitochondrial dysfunction as an arrhythmogenic substrate: a translational proof-of- concept study in patients with metabolic syndrome in whom postoperative atrial fibrillation develops. J Am Coll Cardiol. 2013;62(16):1466–73.
20. Rauniyar N. Parallel Reaction Monitoring: A Targeted Experiment Performed Using High Resolution and High Mass Accuracy Mass Spectrometry. Int J Mol Sci. 2015;16(12):28566–81.
21. Agrawal A, Singh PP, Bottazzi B, Garlanda C, Mantovani A. Pattern recognition by pentraxins. Adv Exp Med Biol. 2009;653:98–116.
22. Pilling D, Gomer RH. The Development of Serum Amyloid P as a Possible Therapeutic. Front Immunol. 2018;9:2328.
23. Richards DB, Cookson LM, Barton SV, Liefaard L, Lane T, Hutt DF et al. Repeat doses of antibody to serum amyloid P component clear amyloid deposits in patients with systemic amyloidosis. Sci Transl Med. 2018; 10(422):eaan3128.
24. Xi D, Luo T, Xiong H, Liu J, Lu H, Li M, et al. SAP: structure, function, and its roles in immune-related diseases. Int J Cardiol. 2015;187:20–6.
25. El-Am EA, Dispenzieri A, Melduni RM, et al. Direct Current Cardioversion of Atrial Arrhythmias in Adults With Cardiac Amyloidosis. J Am Coll Cardiol. 2019;73(5):589–97.
26. Zahedi K. Characterization of the binding of serum amyloid P to type IV collagen. J Biol Chem. 1996;271(25):14897–902.
27. Zahedi K. Characterization of the binding of serum amyloid P to laminin. J Biol Chem. 1997;272(4):2143–8.
28. Jiang YY, Hou HT, Yang Q, Liu XC, He GW. Chloride channels are involved in the development of atrial fibrillation - a transcriptomic and proteomic study. Sci Rep-Uk. 2017;7(1):10215.
29. Worke LJ, Barthold JE, Seelbinder B, Novak T, Main RP, Harbin SL et al. Densification of type I collagen matrices as a model for cardiac fibrosis. Adv Healthc Mater. 2017; 6(22):10.1002/adhm.201700114.
30. Gajko-Galicka A. Mutations in type I collagen genes resulting in osteogenesis imperfecta in humans. Acta Biochim Pol. 2002;49(2):433–41.
31. Ravassa S, Ballesteros G, López B, Ramos P, Bragard J, González A, et al. Combination of circulating type I collagen-related biomarkers is associated with atrial fibrillation. J Am Coll Cardiol. 2019;73(12):1398–410.
32. Schotten U, Verheule S, Kirchhof P, Goette A. Pathophysiological mechanisms of atrial fibrillation: a translational appraisal. Physiol Rev. 2011;91(1):265–325.
33. Chen HX, Li MY, Jiang YY, Hou HT, Wang J, Liu XC, et al. Role of the PPAR pathway in atrial fibrillation associated with heart valve disease: transcriptomics and proteomics in human atrial tissue. Signal Transduct Target Ther. 2020;5(1):4.
34. Li MY, Chen HX, Hou HT, Wang J, Liu XC, Yang Q, et al. Biomarkers and key pathways in atrial fibrillation associated with mitral valve disease identified by multi-omics study. Ann Transl Med. 2021;9(5):393.

Publisher's note